Holocene sea level instability in the southern Great Barrier Reef, Australia: high-precision U–Th dating of fossil microatolls

Nicole D. Leonard, J-x Zhao, K. J. Welsh, Y-x Feng, S. G. Smithers, J. M. Pandolfi & T. R. Clark

Coral Reefs
Journal of the International Society for Reef Studies

ISSN 0722-4028

Coral Reefs
DOI 10.1007/s00338-015-1384-x

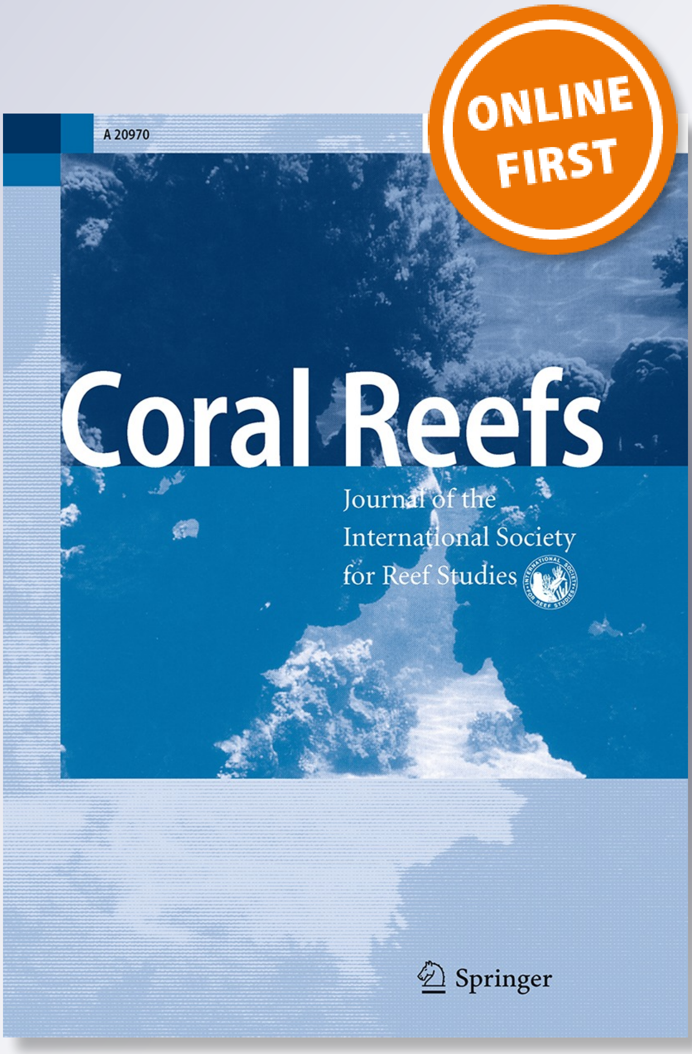

Springer

Coral Reefs
DOI 10.1007/s00338-015-1384-x

REPORT

Holocene sea level instability in the southern Great Barrier Reef, Australia: high-precision U–Th dating of fossil microatolls

Nicole D. Leonard[1,2] · J-x Zhao[1,2] · K. J. Welsh[1] · Y-x Feng[1,2] · S. G. Smithers[3] · J. M. Pandolfi[4] · T. R. Clark[1,2]

Received: 25 August 2015 / Accepted: 1 December 2015

Abstract Three emergent subfossil reef flats from the inshore Keppel Islands, Great Barrier Reef (GBR), Australia, were used to reconstruct relative sea level (RSL). Forty-two high-precision uranium–thorium (U–Th) dates obtained from coral microatolls and coral colonies (2σ age errors from ± 8 to 37 yr) in conjunction with elevation surveys provide evidence in support of a nonlinear RSL regression throughout the Holocene. RSL was as least 0.75 m above present from $\sim$6500 to 5500 yr before present (yr BP; where "present" is 1950). Following this highstand, two sites indicated a coeval lowering of RSL of at least 0.4 m from 5500 to 5300 yr BP which was maintained for $\sim$200 yr. After the lowstand, RSL returned to higher levels before a 2000-yr hiatus in reef flat corals after 4600 yr BP at all three sites. A second possible RSL lowering event of $\sim$0.3 m from $\sim$2800 to 1600 yr BP was detected before RSL stabilised $\sim$0.2 m above present levels by 900 yr BP. While the mechanism of the RSL instability is still uncertain, the alignment with previously reported RSL oscillations, rapid global climate changes and mid-Holocene reef "turn-off" on the GBR are discussed.

Keywords Sea level · Holocene · Great Barrier Reef · Microatoll · Uranium–thorium · Reef hiatus

Communicated by Geology Editor Prof. Chris Perry

Electronic supplementary material The online version of this article (doi:10.1007/s00338-015-1384-x) contains supplementary material, which is available to authorized users.

✉ Nicole D. Leonard
nicole.leonard@uqconnect.edu.au

1 School of Earth Sciences, The University of Queensland, St Lucia, Australia

2 Radiogenic Isotope Facility, The University of Queensland, St Lucia, Australia

3 School of Earth and Environmental Sciences, James Cook University, Townsville, Australia

4 Australian Research Council Centre of Excellence for Coral Reef Studies, Centre for Marine Science, School of Biological Sciences, The University of Queensland, St Lucia, Australia

Introduction

It is indisputable that coral reefs are under increasing pressure from anthropogenic influence globally (Pandolfi et al. 2003; Veron et al. 2009). Nevertheless, natural processes have equally affected reef development throughout geological history, and coral reefs worldwide have suffered significant disturbances and hiatuses prior to anthropogenic influence (Buddemeier and Hopley 1988; Hughes and Connell 1999; Smithers et al. 2006; Perry and Smithers 2011; Hamanaka et al. 2012; Toth et al. 2012). Determining the driving mechanisms of previous reef disturbance events is not only vital to interpreting Holocene reef histories, but allows for improved understanding of the future trajectory of reefs under changing climatic and environmental conditions.

Eustatic sea level (ESL) transgressive/regressive cycles are one of the primary controls of coral reef expansion/contraction throughout the Quaternary (Kennedy and Woodroffe 2002; Hopley et al. 2007). Whereas ESL is dominated by changes in ice sheet volume and global steric variations, relative sea level (RSL) at any given coastline is governed by ESL contributions, as well as regional glacio-hydro-isostatic and tectonic effects (Lambeck and Nakada 1990; Lambeck 1993; Lambeck et al. 2014), water redistribution (Mitrovica and Milne 2002) and climate

Published online: 14 December 2015

(Hamanaka et al. 2012). At near-field sites (close to former ice sheets and melt water), glacio-isostatic influence on RSL is dominant; however, at far-field locations (distant from major ice accumulations), RSL at centennial to millennial timescales is mainly controlled by hydro-isostasy, equatorial ocean syphoning and steric effects which can produce significant spatial and temporal variability over just a few hundred kilometres (Lambeck and Nakada 1990; Mitrovica and Milne 2002).

Geophysical modelling of the regional response to glacio-hydro-isostatic processes has resulted in the identification of distinct zones of globally predicted RSL throughout the Holocene (Clark et al. 1978; Pirazzoli and Pluet 1991). The islands and reefs of the inshore Great Barrier Reef (GBR), proximal to the mainland Queensland coast are characterised by rapidly rising RSL from the early to mid-Holocene, culminating in a RSL highstand of +1 to +3 m by ~5000 yr before present, after which significant meltwater contribution from the large northern hemisphere ice sheets ceased (Clark et al. 1978; Nakada and Lambeck 1989). Evidence of this highstand along the Australian east coast (AEC) between 7000 and 5000 yr before present (yr BP; where "present" is 1950) is widespread and widely accepted (Hopley 1980; Chappell et al. 1982; Chappell 1983; Woodroffe et al. 2000; Lewis et al. 2008; Yu and Zhao 2010; Leonard et al. 2013), although the magnitude and precise timing of the highstand are yet to be unequivocally refined (see Lewis et al. 2008, 2013 for comprehensive reviews of Australian sea level throughout the Holocene).

Inshore reef development on the GBR reflects the rapid early to mid-Holocene RSL rise with coral initiation following inundation of the shallow Pleistocene shelf from ~8500 yr BP, followed by rapid reef accretion in either "catch up" or "keep up" modes of growth until ~5500 yr BP (Neumann and Macintyre 1985; Kleypas and Hopley 1992; Smithers et al. 2006; Perry and Smithers 2011; Camoin and Webster 2015). After ~5500 yr BP, however, both RSL and reef growth histories become increasingly ambiguous. Whether RSL regressed smoothly (Chappell 1983) or oscillated/stepped down (Baker and Haworth 2000; Baker 2001; Lewis et al. 2008) on the AEC following the mid-Holocene highstand has been a contentious issue for over four decades. Indeed, different statistical treatments of the same sea level (SL) data suggest that either regression mode is equally likely (Woodroffe 2009). At the same time, stratigraphic hiatuses in coral reef cores and a lack of reef initiation in the northern and southern inshore GBR have been documented from 5500 to 2800 yr BP, suggestive of significant environmental change at this time (Perry and Smithers 2011). Perry and Smithers (2011) proposed that a reduction in vertical accommodation space due to slowly falling RSL in synergy with changes to environmental conditions at inshore locations (e.g., temperature, rainfall and shore progradation) limited significant reef aggradation/progradation in the mid-Holocene. However, such a synchronous and broad-scale response is suggestive of either a more abrupt change in RSL than currently proposed for the GBR (Chappell 1983), or that rapid and wide-scale climatic and environmental change was the primary driver of reef "turn-off" (Buddemeier and Hopley 1988).

While rapid changes or oscillations in RSL during the Holocene have been proposed for the AEC, they are most often dismissed as artefacts of the proxies used and uncertainties of age error calculations (Perry and Smithers 2011). To obtain a temporally continuous record, it is often necessary to incorporate dissimilar SL indicators, or SL indicators from large latitudinal ranges, into a single interpretation potentially obscuring subtle variations (Chappell 1983; Sloss et al. 2007; Lewis et al. 2008, 2013). Additionally, directly comparing or combining data from separate studies is problematic as: (1) the reference datum and the absolute elevation of the indicators used may differ; (2) inconsistent methods between studies are used to establish elevation and age; (3) large age errors may be associated with dating techniques, e.g., for ^{14}C dating, substantial age errors up to ±500 yr may be introduced if temporal changes in atmospheric production rates as well as global and regional marine ^{14}C reservoir effects are taken into consideration (McGregor et al. 2008; Yu et al. 2010; Hua et al. 2015); and (4) the environmental context of the indicators is critically important but is often difficult to interpret and commonly not reported.

The primary objective of this study was to determine whether low-magnitude RSL instability could be detected using highly precise uranium–thorium (U–Th) dating techniques from multiple sites in a tectonically stable far-field region. To refine our interpretation, we used a single SL proxy (coral microatolls) from multiple reefs in the same region. In addition, we obtained samples of non-microatolls to relate dated microatolls to reef flat development at their time of growth. This sampling regime allowed for both intra- and inter-site comparisons of equivalent data, thereby increasing the confidence in the absolute RSL signal versus single reef geomorphological effects. This study is the first comprehensive evaluation of Holocene RSL and reef flat history in the Keppel Islands, a region for which data have been notably absent (Hopley et al. 2007; Lewis et al. 2013).

Materials and methods

Regional setting

The Keppel Islands are a group of continental islands located on the inner shelf of the southern GBR, Queensland, Australia (23°10′S, 150°59′E; Fig. 1). The islands are located in a macro-tidal setting with a maximum tidal range of ~5 m. The region experiences a seasonally dry tropical climate in which most (on average 60 %) of the rainfall typically occurs in the short wet season between December and March (Bureau of Meteorology 2011). Inter-annual variability is also high, with long dry periods often followed by episodic high rainfall associated with tropical cyclones or monsoonal lows (Brooke et al. 2008) which are modulated by complex interactions between the El Niño Southern Oscillation (ENSO) and Pacific Decadal Oscillation (Rodriguez-Ramirez et al. 2014). Due to frequent disturbance events (e.g., cyclones, flood plumes), the modern Keppel Islands reefs are dominated by fast-growing arborescent *Acropora* spp. (Electronic Supplementary Material, ESM S1 Keppel Islands).

Three islands with evident emergent reef flats containing fossil corals and microatolls in growth position were visited from 19 to 23 June 2013 at low tide: North Keppel Island (NKI); Great Keppel Island (GKI); and Humpy Island (HI; Fig. 1). All sites had seaward-sloping reef flats with no evidence of significant reef rims. Microatolls of various sizes (diameter range 40–250 cm; Fig. 2; Table 1) were targeted to allow for the detection of possible shorter phases of RSL instability that may not be recognised if only the largest microatolls were sampled. The elevation of the microatolls above the fossil reef substrate was up to 0.4 m but much of the former substrate was overlain by thick unconsolidated mixed siliciclastic/carbonate sediments (Fig. 2a) or infilled with authogenic carbonate sands (Fig. 2d). At HI (microatolls $n = 12$; non-microatolls $n = 10$) and GKI (microatolls $n = 8$), elevations were taken using a Magnum-Proshot 4.7 laser level and Apache Lightning 2 receiver and referenced against replicate timed-still tide levels. Due to limited time to access the reef flat at low tide at NKI, microatolls ($n = 13$) were measured directly against still water level within groups that had elevation differences <5 cm. All elevations were determined using tide gauge data from Rosslyn Bay (Station-

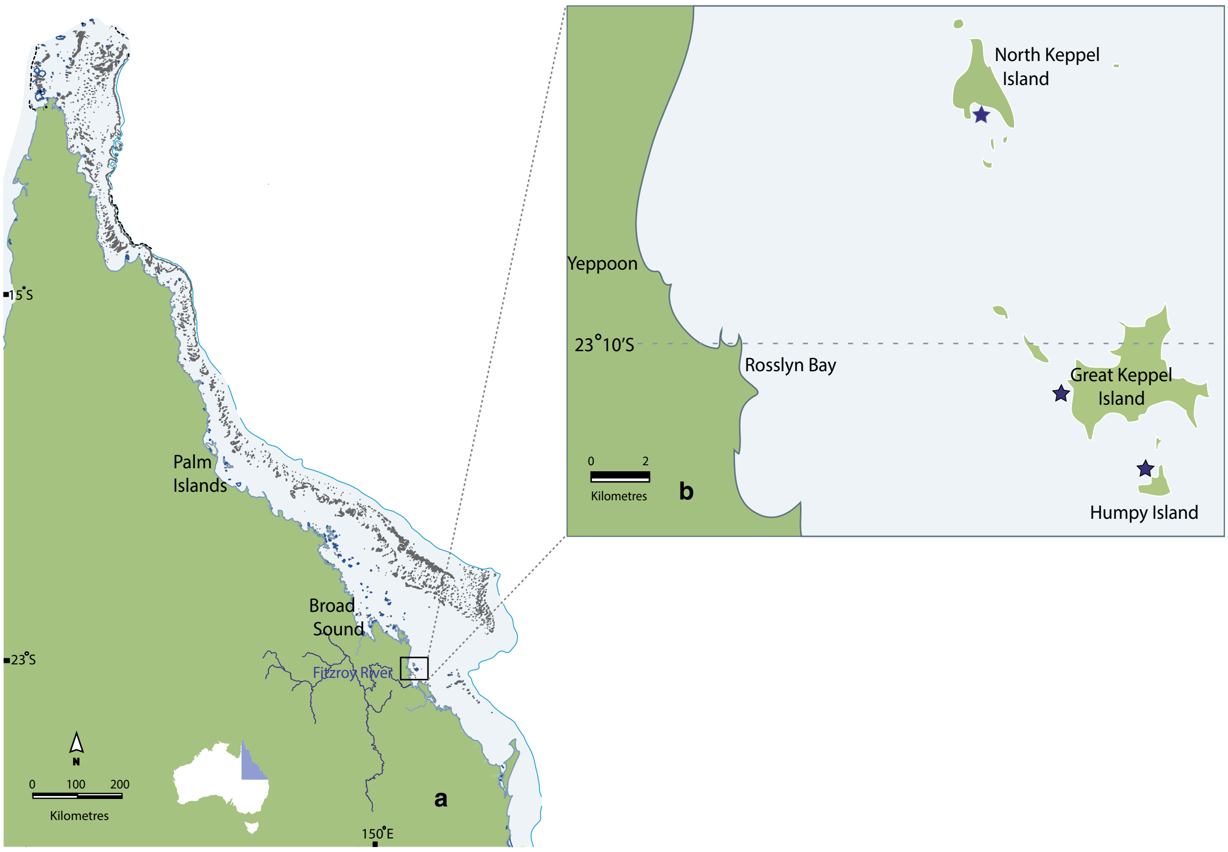

Fig. 1 **a** Queensland, Australia, showing the Great Barrier Reef (*in grey*) and the location of the Keppel Islands. *Blue line* is 200 m isobath; the continental shelf is *shaded in blue*. **b** Locations of the Keppel Islands (North Keppel, Great Keppel and Humpy Islands) and fossil reef flat sites (*black stars*)

Fig. 2 **a** Microatoll at Great Keppel Island. Note thick unconsolidated sediment surrounding sample. **b** Modern reef seaward of relict reef at Great Keppel Island dominated by branching *Acropora* spp. **c** Surface morphology of *Cyphastrea* sp. microatoll demonstrating radiation of corallites from the centre of the colony. **d** Large microatoll at the seaward edge of North Keppel Island reef (survey rod is ~1.3 m)

024011A; Fig. 1) provided by Maritime Safety Queensland and reduced to metres relative to present which we defined as the height above local mean low water spring tide (MLWS; 0.76 m above lowest astronomical tide for the Keppel Islands), the level to which microatolls are constrained by the air–sea interface (Scoffin et al. 1978; Smithers and Woodroffe 2000; Murray-Wallace and Woodroffe 2014).

Even though conditions were calm on all days (<5 knot winds; mean sea level pressure MSLP ~1000 hPa), we acknowledge that measuring the absolute elevation of microatolls by referencing to timed-still tide levels is imprecise, mainly related to possible time lags between tide gauge location and our sites. Although the difference in tide time in the Keppel Islands is only ±5 min from the mainland (which was taken into consideration when calculating heights), to avoid underestimating methodological errors we calculated the average standard deviation of tide heights within a half-hour period of our sea level tie points, which resulted in errors of <0.1 m. The standard deviation of replicate tie points at each site was <0.05 m even when the time difference was in excess of an hour between measurements. We therefore assigned a conservative error of ±15 cm to our measurements to incorporate both sources of potential error. It must be noted, however, that the error of the relative position of each coral sample to each other within each site is minimal and is a function of the laser level (accuracy of ±1.0 mm/30 m; HI and GKI) or relative position to each other (<0.05 m; NKI).

Samples of coral were collected with a hammer and chisel from the centre of each coral microatoll where the elevation and diameter were recorded (Table 1). Samples were also taken from the centre of non-microatoll fossil colonies at HI ($n = 10$) to determine reef flat development.

Table 1 Results of MC-ICP-MS uranium–thorium dating and elevation surveys of fossil microatolls from the Keppel Islands, Southern Great Barrier Reef, Australia

Sample name	U (ppm)	^{232}Th (ppb)	(^{230}Th/^{232}Th)	(^{230}Th/^{238}U)	(^{234}U/^{238}U)	Uncorr. Age[a]	Corr. Age[b]
HUMP 001	2.8147 ± 0.0017	1.3017 ± 0.0028	385.5 ± 1.7	0.05875 ± 0.00024	1.1435 ± 0.0013	5753 ± 25	5739 ± 25
HUMP 002	2.6366 ± 0.0018	0.1065 ± 0.0012	4294 ± 49	0.05705 ± 0.00019	1.1449 ± 0.007	5576 ± 19	5570 ± 19
HUMP 003	3.3272 ± 0.0024	1.6978 ± 0.0025	364.9 ± 1.6	0.61366 ± 0.00026	1.1436 ± 0.0010	6015 ± 27	6002 ± 27
HUMP 004	3.3226 ± 0.0024	7.366 ± 0.013	82.5 ± 0.3	0.06026 ± 0.00021	1.1449 ± 0.0009	5898 ± 22	5849 ± 25
HUMP 006	3.4795 ± 0.0013	2.4757 ± 0.0038	227.4 ± 1.0	0.05332 ± 0.00021	1.1422 ± 0.0010	5215 ± 21	5197 ± 22
HUMP 007	3.5303 ± 0.0017	1.4009 ± 0.0021	404.0 ± 1.4	0.05284 ± 0.00017	1.1436 ± 0.0011	5161 ± 18	5149 ± 18
HUMP 008	3.0912 ± 0.0027	2.3010 ± 0.0044	225.2 ± 1.2	0.05525 ± 0.00028	1.1437 ± 0.0011	5402 ± 28	5382 ± 29
HUMP 009	3.3431 ± 0.0019	5.5019 ± 0.0075	112.5 ± 0.5	0.06104 ± 0.00024	1.1455 ± 0.0010	5973 ± 24	5930 ± 32
HUMP 010	3.4909 ± 0.0021	3.6409 ± 0.0049	205.6 ± 0.7	0.07067 ± 0.00023	1.1442 ± 0.0009	6953 ± 24	6928 ± 25
HUMP 011	2.8329 ± 0.0018	0.4291 ± 0.0015	1283.4 ± 6.8	0.06407 ± 0.00026	1.1449 ± 0.0012	6281 ± 27	6273 ± 27
HUMP 012	3.0712 ± 0.0014	1.2108 ± 0.0022	514.7 ± 2.0	0.06688 ± 0.00022	1.1440 ± 0.0010	6570 ± 23	6558 ± 24
HUMP 013	3.0504 ± 0.0022	12.409 ± 0.021	48.6 ± 0.2	0.06519 ± 0.00029	1.1443 ± 0.0009	6398 ± 30	6310 ± 37
HUMP 014	3.1765 ± 0.0019	6.4363 ± 0.0087	95.8 ± 0.4	0.06395 ± 0.00026	1.1443 ± 0.0011	6272 ± 27	6227 ± 29
HUMP 015	3.5019 ± 0.0016	2.3805 ± 0.0042	298.8 ± 1.3	0.06694 ± 0.00028	1.1437 ± 0.0007	6579 ± 28	6561 ± 28
HUMP 016	3.5124 ± 0.0021	2.8456 ± 0.0033	248.9 ± 0.8	0.06645 ± 0.00022	1.1448 ± 0.0009	6522 ± 23	6502 ± 23
HUMP 017	3.3614 ± 0.0021	2.2358 ± 0.0039	265.5 ± 0.9	0.05820 ± 0.00017	1.1426 ± 0.0009	5702 ± 18	5685 ± 18
HUMP 018	2.8587 ± 0.0014	0.4336 ± 0.0012	219.2 ± 1.9	0.010959 ± 0.000090	1.1468 ± 0.0007	1048 ± 9	1041 ± 9
HUMP 019	3.0813 ± 0.0014	0.4114 ± 0.0014	246.7 ± 2.0	0.010854 ± 0.000080	1.1460 ± 0.0013	1039 ± 8	1032 ± 8
HUMP 020	3.4097 ± 0.0015	0.4805 ± 0.0014	1176.3 ± 6.3	0.05464 ± 0.00025	1.1463 ± 0.0011	5328 ± 25	5321 ± 25
HUMP 021	2.7724 ± 0.0017	0.054188 ± 0.00066	9150 ± 120	0.05867 ± 0.00023	1.1449 ± 0.0012	5739 ± 24	5734 ± 24
HUMP 022	3.2932 ± 0.0014	1.8478 ± 0.0023	327.9 ± 1.3	0.06065 ± 0.00024	1.1452 ± 0.0007	5935 ± 24	5920 ± 24
HUMP 023	3.5361 ± 0.0016	1.2274 ± 0.0019	546.7 ± 2.0	0.06254 ± 0.00021	1.1456 ± 0.0008	6123 ± 21	6112 ± 21
NKI 001	3.1841 ± 0.0022	0.5042 ± 0.0016	1018.0 ± 6.0	0.05313 ± 0.00027	1.1422 ± 0.0008	5196 ± 27	5189 ± 27
NKI 002	2.8433 ± 0.0014	7.5792 ± 0.0084	63.9 ± 0.2	0.05615 ± 0.00017	1.1457 ± 0.0010	5482 ± 18	5423 ± 23
NKI 003	2.9487 ± 0.0011	0.0203 ± 0.0010	2238 ± 14	0.05082 ± 0.00018	1.1434 ± 0.0008	4960 ± 18	4954 ± 18
NKI 004	3.2567 ± 0.0015	2.5073 ± 0.0039	205.9 ± 0.9	0.05224 ± 0.00021	1.1438 ± 0.0010	5101 ± 21	5081 ± 21
NKI 005	3.2033 ± 0.0014	3.7824 ± 0.0044	134.1 ± 0.5	0.05218 ± 0.00018	1.1448 ± 0.0009	5089 ± 19	5061 ± 20
NKI 006	2.6269 ± 0.0012	0.2884 ± 0.0014	1382.9 ± 9.6	0.05004 ± 0.00024	1.1454 ± 0.0008	4874 ± 25	4867 ± 25
NKI 007	3.2162 ± 0.0011	0.2171 ± 0.0011	2202 ± 15	0.04899 ± 0.00020	1.1450 ± 0.0010	4770 ± 21	4764 ± 21
NKI 008	3.2828 ± 0.0016	10.544 ± 0.013	50.1 ± 0.2	0.05303 ± 0.00025	1.1442 ± 0.0010	5177 ± 25	5108 ± 30
NKI 009	2.9348 ± 0.0012	3.4989 ± 0.0050	130.6 ± 0.5	0.05132 ± 0.00018	1.1443 ± 0.0010	5006 ± 19	4977 ± 20
NKI 010	2.7258 ± 0.0012	0.5414 ± 0.0016	792.8 ± 4.7	0.05189 ± 0.00027	1.1448 ± 0.0008	5061 ± 27	5052 ± 27
NKI 011	3.2569 ± 0.0014	0.0837 ± 0.0010	5687 ± 72	0.04819 ± 0.00020	1.1475 ± 0.0008	4680 ± 20	4676 ± 20
NKI 012	2.7301 ± 0.0015	3.1752 ± 0.0039	158.5 ± 0.7	0.06075 ± 0.00024	1.1448 ± 0.0010	5948 ± 25	5919 ± 26

Table 1 continued

Sample name	U (ppm)	^{232}Th (ppb)	(^{230}Th/^{232}Th)	(^{230}Th/^{238}U)	(^{234}U/^{238}U)	Uncorr. Age[a]	Corr. Age[b]
NKI 013	2.8941 ± 0.0011	0.3032 ± 0.0011	1716 ± 10	0.05925 ± 0.00027	1.1452 ± 0.0008	5795 ± 27	5789 ± 27
GKI 001	3.2827 ± 0.0012	2.3108 ± 0.0033	131.0 ± 0.6	0.03039 ± 0.00015	1.1445 ± 0.0007	2938 ± 15	2919 ± 15
GKI 002	3.1006 ± 0.0012	11.496 ± 0.017	14.5 ± 0.1	0.01772 ± 0.00012	1.1456 ± 0.0009	1702 ± 12	1623 ± 23
GKI 003	2.9822 ± 0.0011	4.4127 ± 0.0058	33.5 ± 0.3	0.01632 ± 0.00012	1.1456 ± 0.0008	1566 ± 12	1532 ± 15
GKI 004	2.7803 ± 0.0010	1.4822 ± 0.0023	96.6 ± 0.7	0.01698 ± 0.00012	1.1482 ± 0.0011	1626 ± 12	1611 ± 13
GKI 005	3.1125 ± 0.0010	7.356 ± 0.011	23.5 ± 0.2	0.01827 ± 0.00011	1.1448 ± 0.0009	1756 ± 11	1704 ± 17
GKI 007#	3.1193 ± 0.0010	25.717 ± 0.034	6.8 ± 0.1	0.01859 ± 0.00014	1.1478 ± 0.0007	1783 ± 14	1611 ± 45
GKI 008	3.0879 ± 0.0013	2.3435 ± 0.0033	110.8 ± 0.4	0.02770 ± 0.00010	1.1456 ± 0.0009	2672 ± 10	2652 ± 11
GKI 009	3.0791 ± 0.0014	0.7192 ± 0.0014	867.2 ± 4.1	0.06676 ± 0.00029	1.1442 ± 0.0010	6557 ± 30	6548 ± 30

Sample name	Age (yr BP—1950)	initial δ^{234}U[c]	Genus/growth form (*)	Coral diam (cm)	Elevation (m)	Latitude	Longitude
HUMP 001	5676 ± 25	145.9 ± 1.3	Leptastrea	85	0.66	23°12′46.4	150°58′10.8
HUMP 002	5507 ± 19	147.2 ± 0.7	Cyphastrea	150	0.64	23°12′46.4	150°58′11.0
HUMP 003	5939 ± 27	143.6 ± 1.0	Pavona*	120	0.23	23°12′45.9	150°58′09.5
HUMP 004	5785 ± 25	147.4 ± 0.9	Branching*	180	0.46	23°12′46.8	150°58′10.5
HUMP 006	5134 ± 22	144.4 ± 1.0	Porites	250	0.16	23°12′46.0	150°58′08.6
HUMP 007	5086 ± 18	145.7 ± 1.1	Porites	70	0.09	23°12′45.9	150°58′08.6
HUMP 008	5319 ± 29	145.9 ± 1.1	Porites	75	0.2	23°12′45.8	150°58′08.9
HUMP 009	5867 ± 32	145.6 ± 1.0	Pavona*	110	0.19	23°12′45.6	150°58′09.7
HUMP 010	6864 ± 25	147.1 ± 1.0	Branching*	250	0.1	23°12′44.1	150°58′10.1
HUMP 011	6209 ± 27	147.5 ± 1.2	Cyphastrea	75	0.4	23°12′44.4	150°58′10.7
HUMP 012	6495 ± 24	146.7 ± 1.0	Porites cylindrica*	90	0.46	23°12′44.4	150°58′11.0
HUMP 013	6247 ± 37	147.1 ± 0.9	Porites cylindrica*	110	0.58	23°12′44.9	150°58′11.5
HUMP 014	6163 ± 29	147.0 ± 1.1	Porites cylindrica*	210	0.58	23°12′44.8	150°58′11.4
HUMP 015	6497 ± 28	146.4 ± 0.7	Porites cylindrica*	70	0.59	23°12′45.1	150°58′11.3
HUMP 016	6438 ± 23	147.5 ± 0.9	Porites cylindrica*	100	0.64	23°12′45.3	150°58′11.3
HUMP 017	5621 ± 18	145.0 ± 0.9	Porites cylindrica*	200	0.1	23°12′46.8	150°58′07.7
HUMP 018	977 ± 9	147.3 ± 0.7	Cyphastrea	230	0.1	23°12′47.9	150°58′08.2
HUMP 019	968 ± 8	146.4 ± 1.3	Cyphastrea	170	0.2	23°12′46.7	150°58′08.5
HUMP 020	5257 ± 25	148.6 ± 1.1	Porites	150	0.3	23°12′47.1	150°58′08.7
HUMP 021	5670 ± 24	147.2 ± 1.3	Cyphastrea	180	0.7	23°12′46.4	150°58′11.1
HUMP 022	5856 ± 24	147.6 ± 0.7	Porites	210	0.66	23°12′46.4	150°58′11.0
HUMP 023	6048 ± 21	148.2 ± 0.8	Leptastrea	130	0.68	23°12′46.2	150°58′11.0
NKI 001	5125 ± 27	144.3 ± 0.8	Porites	250	0.39	23°04′57.6	150°53′52.8
NKI 002	5359 ± 23	148.0 ± 1.0	Porites	120	0.39	23°04′57.6	150°53′52.2
NKI 003	4891 ± 18	145.5 ± 0.8	Cyphastrea	70	0.63	23°04′52.7	150°53′51.7

Table 1 continued

Sample name	Age (yr BP—1950)	initial $\delta^{234}U^{c}$	Genus/growth form (*)	Coral diam (cm)	Elevation (m)	Latitude	Longitude
NKI 004	5017 ± 21	145.9 ± 1.0	Porites	110	0.63	23°04′52.4	150°53′51.6
NKI 005	4997 ± 20	147.0 ± 1.0	Porites	100	0.63	23°04′52.4	150°53′51.1
NKI 006	4803 ± 25	147.4 ± 0.8	Favites	90	0.73	23°04′50.5	150°53′50.8
NKI 007	4701 ± 21	147.0 ± 1.0	Cyphastrea	100	0.73	23°04′49.8	150°53′50.9
NKI 008	5044 ± 30	146.4 ± 1.0	Porites	90	0.73	23°04′49.6	150°53′50.9
NKI 009	4913 ± 20	146.4 ± 1.0	Porites	80	0.73	23°04′49.2	150°53′50.6
NKI 010	4988 ± 27	146.9 ± 0.8	Favites	160	0.77	23°04′48.5	150°53′49.3
NKI 011	4612 ± 20	149.5 ± 0.8	Cyphastrea	120	0.77	23°04′48.4	150°53′48.9
NKI 012	5856 ± 26	147.2 ± 1.0	Porites	200	0.77	23°04′48.0	150°53′49.0
NKI 013	5725 ± 27	147.6 ± 0.8	Cyphastrea	140	0.79	23°04′47.1	150°53′49.3
GKI 001	2856 ± 15	145.7 ± 0.7	Porites	130	0.29	23°11′48.2	150°56′19.4
GKI 002	1559 ± 23	146.3 ± 0.9	Porites	90	0.1	23°11′47.8	150°56′18.8
GKI 003	1468 ± 15	146.3 ± 0.8	Porites	130	0.17	23°11′47.3	150°56′19.5
GKI 004	1547 ± 13	148.9 ± 1.1	Cyphastrea	150	0.05	23°11′45.9	150°56′19.8
GKI 005	1640 ± 17	145.6 ± 0.9	Porites	50	−0.07	23°11′44.9	150°56′19.6
GKI 007#	1548 ± 45	147.9 ± 0.9	Porites	70	0.12	23°11′46.0	150°56′20.1
GKI 008	2588 ± 11	146.7 ± 0.9	Cyphastrea	100	0.2	23°11′45.4	150°56′21.4
GKI 009	6484 ± 30	146.9 ± 1.1	Goniastrea	40	0.52	23°11′45.3	150°56′24.0

Ratios in parentheses are activity ratios calculated from atomic ratios using decay constants of Cheng et al. (2000). All values have been corrected for laboratory procedural blanks. All errors reported in this table are quoted as 2σ

* Indicates non-microatoll

Sample removed from analysis

[a] Uncorrected ^{230}Th age was calculated using Isoplot/EX 3.0 program (Ludwig 2003)

[b] ^{230}Th ages were corrected using the two-component correction method of Clark et al. (2014a) using $^{230}Th/^{232}Th_{hyd}$ and $^{230}Th/^{232}Th_{det}$ activity ratios of 1.08 ± 0.23 and 0.62 ± 0.14, respectively

[c] $\delta^{234}U = [(^{234}U/^{238}U) - 1] \times 1000$

The flat, upper surface of the centre of the coral microatoll where the corallites were observed to radiate (Fig. 2c) represents the surface of the colony that was originally constrained by the air–sea interface and was used to justify our sampling strategy. Furthermore, personal observations and previous dating trials have revealed that the centres of microatolls and corals are generally less prone to bio-erosion and detrital inclusions allowing for more precise U–Th age determinations.

Uranium–thorium dating

Samples were prepared for U–Th dating by Multi-Collector Inductively Coupled Mass Spectrometry (MC-ICP-MS) at the Radiogenic Isotope Facility, the University of Queensland, using methods described in Clark et al. (2012, 2014b). Full laboratory methods are described in detail in ESM S2 U–Th methods. Samples of coeval material with different levels of cleaning protocol were measured for age validation of replicate samples and to determine local detrital $^{230}Th/^{232}Th$ ratios using $^{230}Th/^{232}Th$–$^{238}U/^{232}Th$ isochrons (ESM Fig. S1). Sample ages were calculated using the decay constants of Cheng et al. (2000) using Isoplot/Ex software (Ludwig 2003) and corrected for initial/detrital ^{230}Th using a two-component mixing correction scheme described by Clark et al. (2014a).

Results

Uranium–thorium age data

Measured ^{232}Th for the corals collected from the Keppel Islands was variable, with 98 % of samples ranging 0.08–12.41 ppb (72 % <3.5 ppb) suggesting small to negligible initial ^{230}Th and/or non-radiogenic detrital ^{230}Th contamination in most of the samples collected (Table 1). Elevated ^{232}Th (25.72 ppb) and a low $^{230}Th/^{232}Th$ ratio (6.84) were determined for sample GKI007, indicating significant contamination with detrital ^{230}Th and justifying the removal of this sample from further analysis (removal of this data point did not affect interpretation). All samples appear to have remained a closed system supported by $\delta^{234}U$ values falling within analytical error of the modern seawater value of 146.8 ± 2 ‰ and uranium concentrations similar to previously reported values for pristine coral, ranging 2.6–3.5 ppm (Henderson 2002; Cobb et al. 2003; Shen et al. 2008; Clark et al. 2012; Leonard et al. 2013). The average detrital $^{230}Th/^{232}Th$ ratio obtained from the Keppel Islands isochrons (0.62 ± 0.14; ESM Fig. S1) is close to the 0.64 ± 0.04 ratio reported by Clark et al. (2014a) for massive *Porites* colonies at the Palm Islands (Fig. 1), a comparable inshore site ~650 km north of the Keppel Islands. Three replicate isochron samples used for age validation (GKI003, GKI004 and GKI005) are all within age error of the reported U–Th age of the final ultra-cleaned sample (ESM Fig. S2).

Age elevation

Keppel Islands corrected ^{230}Th ages of corals and microatolls [$n = 42$; reported hereafter as years before present (1950)] ranged from 6864 to 968 yr BP, although distributed discontinuously throughout this time (Table 1). Reef flats had developed at all three sites by the mid-Holocene, yet no reef flat samples at any site were dated between ~4600 and 2800 yr BP. All elevations are reported relative to MLWS tide height to which open-water microatolls are constrained and therefore considered representative of height above/below present RSL.

Humpy Island is the smallest island and reef flat of the three sites investigated in this study. The modern leeward reef lies 150–350 m from the emerged reef flat, which is situated in a small embayment on the southwest of the island (Fig. 1; ESM Fig. S3). The oldest microatoll at this site was *Cyphastrea* spp. (6209 ± 27 yr BP) at 0.4 m above present; however, large branching corals were present as early as 6800 yr BP (Fig. 3; Table 1). Both microatolls and non-microatolls are found from ~6200 to 5500 yr BP at ~0.7 m above present suggestive of a fully developed reef flat (Fig. 3). Four *Porites* sp. microatolls dated between ~5300 and 5100 yr BP are ~0.4–0.7 m lower than their older counterparts (Fig. 3) with no corals found above this elevation for this period. After 5100 yr BP, only two late Holocene microatolls ~0.2 m above present at ~970 yr BP are found at this site.

On Great Keppel Island (Fig. 1, ESM Fig. S4), the modern reef is located almost perpendicular to a rocky headland at the seaward edge of an embayment on the south-west of the island and is dominated by branching *Acropora* spp. (Fig. 2b). The relict emergent reef is located ~50 m towards the shore from the living coral zone and is partially covered by mixed siliciclastic/carbonate sediment. Only one mid-Holocene sample (GKI 009) was dated at ~6500 yr BP at 0.52 m above present. While more mid-Holocene samples are most likely present at GKI, the occurrence of relatively thick unconsolidated sediments means that they are probably only intermittently exposed (Fig. 2a). The remaining samples from GKI are all late Holocene from 2800 to 1400 yr BP. Microatolls are 0.3 m above present at 2856 yr BP, −0.07 m at 1640 yr BP, 0.05 m at 1550 yr BP and 0.17 m at 1468 yr BP (Fig. 4a).

At North Keppel Island (Fig. 1, ESM S5), modern coral growth is mainly constrained to the reef slope, with small *Acropora* spp. recruits and a few ponded modern

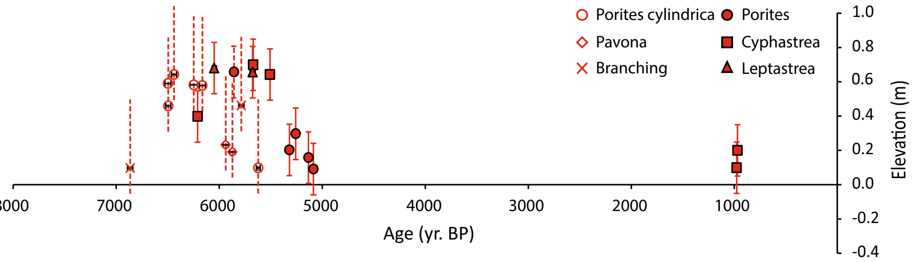

Fig. 3 Uranium–thorium (U–Th) age-elevation data for microatoll and non-microatoll samples from Humpy Island, Great Barrier Reef, Australia. *Solid symbols* are microatolls (elevation errors of ±0.15 m); *open symbols* are non-microatoll samples. As non-microatoll corals are not constrained equally by the air–sea interface, positive elevation errors are given as ≥0.35 m. Elevation is metres (m) above present mean low water spring tide. U–Th ages are years before present (yr BP; "present" = 1950) with errors at 2σ level (note that some age error bars are smaller than symbol width)

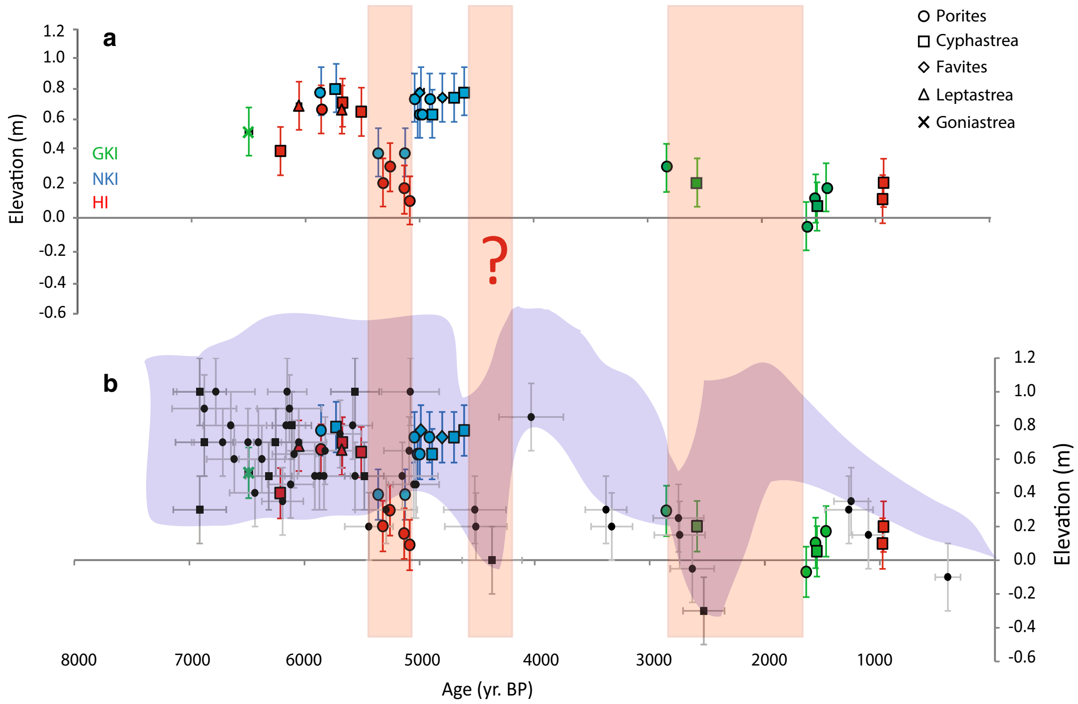

Fig. 4 **a** Uranium–Thorium (U–Th) age-elevation data for microatolls from the Keppel Islands, Great Barrier Reef (GBR), Australia: Great Keppel Island (GKI, *green*), North Keppel Island (NKI, *blue*) and Humpy Island (HI, *red*). Elevation is metres (m) above present mean low water spring tide. U–Th ages are years before present (yr BP; "present" = 1950) with errors at 2σ level (note that some age error bars are smaller than symbol width). **b** Microatoll data from the Keppel Islands (same as [a]) compared to previously published recalibrated (Lewis et al. 2008) microatoll data from the GBR; *black circles*—Chappell (1983) minimum elevation; *grey shaded area*—Lewis et al. (2008) sea level envelope for the Australian east coast. *Shaded red bars* are periods of suggested relative sea level (RSL) oscillations

microatolls (living tissue <5 cm on the edge of the colony; ESM Fig. S6). Fossil microatolls at NKI are ~0.8 m above present sea level from 5800 to 5700 yr BP and 0.4 m above present sea level between 5350 and 5125 yr BP. From 5000 to 4600 yr BP, microatolls are ~0.7 m above present sea level after which no further reef flat corals were found during this study at NKI (Fig. 4a).

Discussion

High-precision U–Th age-elevation data from corals and microatolls in the Keppel Islands provides evidence in support of a nonlinear RSL regression throughout the Holocene on the southern GBR. Our study is based on 42 U–Th dates obtained from in situ fossil microatolls

($n = 32$) and relict reef flat corals ($n = 10$) from three continental islands. This is the first account of centennial-scale RSL instability documented from multiple reefs within the same region.

Mid-Holocene (6500–4600 yr BP)

Models of glacio-hydro-isostatic response of RSL predict a highstand of +1 to +3 m for the inshore GBR in the mid-Holocene (Clark et al. 1978; Chappell et al. 1982; Lambeck and Nakada 1990). The earliest microatoll samples in the Keppel Islands are 0.4–0.5 m above present ~6500–6200 yr BP and ~0.7 m by 6000 yr BP (Figs. 3, 4). Elevations of non-microatoll corals from HI suggest that the highstand was likely reached just after ~6200 yr BP; however, determining absolute RSL from non-microatolls is not possible (Fig. 3a). The highstand in the Keppel Islands is both later and lower than previously proposed highstands on the AEC [e.g., 1.0–1.5 m at 7400 yr BP (Sloss et al. 2007) and 7000 yr BP (Lewis et al. 2008)]. However, these previous highstand data must be treated with caution as they are based on either a limited number of radiocarbon ages obtained from supratidal deposits, for which upper elevation ranges are difficult to determine (Sloss et al. 2007), or recalibrated radiocarbon data from a number of different studies utilising different methods and indicators (Lewis et al. 2008). Early reef initiation in the Keppel Islands may have been inhibited by conditions unsuitable or marginal for coral growth due to the movement of the coastal terrigenous sediment wedge (TSW) and/or resuspension of pretransgressive sediments (Larcombe and Woolfe 1999). Nevertheless, RSL appears not to have peaked in the southern GBR until after 6200 yr BP. Microatoll elevations designate the lower height estimate of RSL, commonly ~0.5 m lower than fixed biological indicators (FBIs, e.g., tubeworms and oyster beds; Lewis et al. 2008) or more when compared to mangrove deposits (Sloss et al. 2007), which makes our data comparable to previous elevation reconstructions.

Following the highstand in the Keppel Islands, two sites (HI and NKI) show a rapid coeval fall in RSL of 0.4–0.7 m at 5500 yr BP, with no microatolls or corals found above 0.4 m between 5300 and 5100 yr BP. This lowering of RSL cannot be explained by a lack of accommodation space as microatolls reform at NKI at higher elevations (0.6–0.7 m) from 5000 to 4600 yr BP at more landward locations on the reef flat (Fig. 5). Although ponding must be considered when interpreting the return to higher RSL after 5100 yr BP, we consider this unlikely. A shore-to-sea survey showed that towards the reef slope the area of highest elevation (potentially causing ponding) is only 0.4 m above present. Thin, ponded extant microatolls (<5 cm above the substrate; ESM Fig. S6) are present on the reef flat at NKI at ~0.4 m above present MLWS, which is still 0.2–0.3 m lower than the microatolls dated between 5000 and 4600 yr BP. The morphology of the modern microatolls also differs from their fossil counterparts with the former defined by planar surfaces formed by very still moated water levels and the latter being vertically more substantial with irregular surfaces (Fig. 2d) indicative of a free-draining reef-flat environment (Smithers and Woodroffe 2000). Though these sites are in a macro-tidal setting, which can result in significant elevation differences among modern microatolls, the precise overlapping (both temporal and magnitudinal) of the lowstand observed at two reef sites makes it extremely unlikely that it is a tidal artefact. If elevation differences in this region were driven primarily by tidal range, our data would consistently show temporally indiscrete elevation differences of >0.3 m throughout the Holocene, which are not apparent.

The timing and magnitude of the sudden RSL lowering in the Keppel Islands agree with FBI data from the southern AEC, which exhibited a RSL fall of ~0.6 m between 5400 and 5000 yr BP (Baker and Haworth 2000; Sloss et al. 2007). Microatoll data from Magnetic Island also indicate that RSL was higher at 5800 yr BP compared to 5400–5000 yr BP (Yu and Zhao 2010). When previously reported (recalibrated; Lewis et al. 2008) microatoll data from the GBR (Chappell 1983) are compared with the Keppel Islands data, the lowered RSL between 5300 and 5100 yr BP is still evident, with samples elevated higher found prior to and following the inferred lowstand (Fig. 4b).

The RSL lowering in the Keppel Islands at 5500 yr BP is also contemporaneous with a period of significant change to reefs on the GBR (Smithers et al. 2006; Lybolt et al. 2011; Perry and Smithers 2011; Leonard et al. 2013). Following the concept of reef "turn on" and "turn-off" events initially proposed by Buddemeier and Hopley (1988), Perry and Smithers (2011) analysed data from 76 reef core records from the inshore GBR and noted that reef initiation ceased from ~5500 yr BP in both the northern (Cape Tribulation; 1000 km north of Keppel Islands) and southern GBR (Cockermouth, Penrith and Scawfell Islands; ~300 km north of Keppel Islands). Similarly, in Moreton Bay (~550 km south of Keppel Islands), sudden reef flat termination (Leonard et al. 2013) and increasing coral depth followed by a reef hiatus (Lybolt et al. 2011) have been documented from ~5600 yr BP. Lack of vertical accommodation space, proximity to the coastal TSW and climate change were suggested as the likely cause of reef "turn-off" (i.e., reduction in accretion) on the inshore GBR (Perry and Smithers 2011). However, it was noted by the authors that similar patterns and/or transitions from aggrading to prograding modes of growth were observed

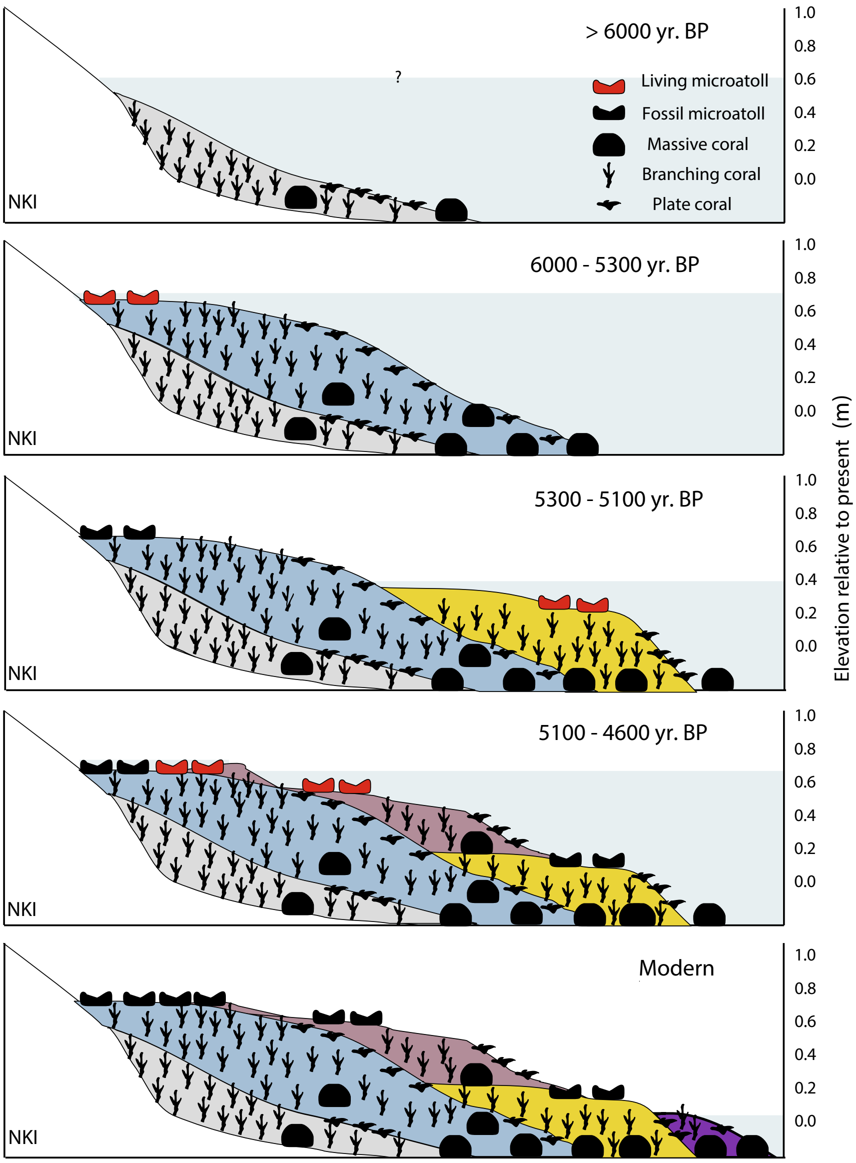

Fig. 5 Schematic of inferred Holocene reef flat development at North Keppel Island, Great Barrier Reef, Australia. Microatoll positions are based on actual position on the reef flat, and reef age is U–Th-derived ages. Elevation is metres relative to present mean low water spring tide. *Red microatoll symbols* represent those being formed at that time period (i.e., living); *black microatoll symbols* represent fossil corals at that time period. *Blue shaded area* represents RSL for each phase. Subsurface corals are an assumption based on general models of reef development, and *different colours* represent inferred reef isochrons

on mid- and outer-shelf reefs far from the effects of terrigenous input or resuspension. In Moreton Bay, a rapid fall in RSL and/or climatic change was suggested to have increased turbidity producing unfavourable conditions for coral growth (Leonard et al. 2013). However, a recent analysis of foraminifer assemblages from Moreton Bay demonstrated that water quality was continuously and consistently marginal from 7400 yr BP to present (Narayan et al. 2015), suggesting that turbidity was likely not the primary driver of reef demise in this region.

The period of reduced accretion ("turn-off") was followed by a significant hiatus in reef growth from ~4600 yr BP that lasted for two millennia (Smithers et al. 2006; Perry and Smithers 2011). Equally, no corals or microatolls were found in the Keppel Islands between 4600 and 2800 yr BP. Previously presented RSL data from the AEC are contradictory, with some authors suggesting that SLs were 1 m (Flood and Frankel 1989) to 1.7 m higher (Baker and Haworth 2000) during this period, whilst others propose possible lowered RSLs at this time (Lewis et al.

2008). The negative RSL oscillation proposed by Lewis et al. (2008) at 4600 yr BP is based on 115 recalibrated ^{14}C SL indicators from the AEC (Fig. 4b). The rate of RSL change calculated from the Keppel Islands microatolls at 5500 yr BP (ESM S5) are comparable to the rates derived from microatolls at 4600 yr BP by Lewis et al. (2008), suggesting similar driving mechanisms for both events. If RSLs were lowered during these periods, sediment loads to inshore reefs would increase due to mainland coastal sedimentary progradation, with flood plumes reaching further across the shelf and increased wave resuspension of fine sediments which may have resulted in significantly reduced reef accumulation or hiatus at some locations as noted by Perry and Smithers (2011). Clearly, more SL proxies that temporally bracket, or are within the GBR hiatus period are needed before any conclusions can be drawn. Nevertheless, the synchronicity of a RSL oscillation at 5500 yr BP and reef flat hiatus at 4600 yr BP in the Keppel Islands with significant reductions in reef initiation and reef hiatus elsewhere on the GBR is noteworthy.

Late Holocene re-initiation (2800 yr BP to present)

Microatoll records suggest that reef flats in the Keppel Islands re-initiated between 2800 and 2500 yr BP, similar to the timing of reef re-initiation (~2300 yr BP) reported in the northern and southern GBR (Perry and Smithers 2011). As only a limited number of samples at GKI and HI were from the late Holocene in the present study, our interpretation is cautious at this stage. Evidence suggests that between 2800 and 2500 yr BP RSL was 0.3–0.2 m above present, after which RSL appears to have been just below or close to present levels by 1640 yr BP. Microatolls are then found at increasing elevations up to 0.2 m above present from 1470 to 970 yr BP. Lewis et al. (2008) proposed a similar oscillation centred at 2800 yr BP at comparable elevations to our present record. More recently, Harris et al. (2015) reported a rapid fall in RSL after ~2200 yr BP at One Tree Island (southern GBR); however, they suggested that RSL was ~1.0 m above present between 3900 and 2200 yr BP. Baker and Haworth (2000) suggested that an absence of succession of various FBIs indicated a rapid RSL fall in Port Hacking (1200 km south of the Keppel Islands) between 3500 and 3400 yr BP, after which RSL was stable until ~2800 yr BP. However, following this period of RSL stability, the Port Hacking data from two sites within the same region displayed divergent trends, one falling and one rising (Baker and Haworth 2000). Perry and Smithers (2011) inferred that reef re-initiation on the GBR during the late Holocene likely occurred due to RSL stabilisation and the associated retreat of the TSW and shoreline resulting in conditions becoming more favourable for accretion. However, data from the Keppel Islands and elsewhere on the GBR and AEC suggest that after 2800 yr BP RSL was unstable at centennial timescales. It is unclear at this stage as to why reefs re-initiated in the late Holocene even if RSL fell smoothly or oscillated.

Mechanisms of RSL oscillations

Neotectonics and hydro-isostasy

The AEC is considered to have been tectonically stable throughout the Holocene (Lambeck and Nakada 1990; Lambeck 2002; Woodroffe and Horton 2005). However, neotectonic uplift of up to 1 m per 1000 yr to the east of the Broad Sound fault (~130 km north of the Keppel Islands) has been suggested (Kleypas and Hopley 1992). At Broad Sound, the continental shelf is at its widest (~200 km) compared with just south of the Keppel Islands where the shelf is approximately three times narrower (~70 km; Fig. 1). It is possible that differential down-warping (i.e., larger effect on the wider shelf) following the mid-Holocene highstand resulted in an increase in tidal range in the Keppel Islands region, which would result in a lowering of the MLWS level without a need for any RSL change or eustatic contribution (Kleypas and Hopley 1992). Although feasible, we consider this unlikely as tidal adjustment would likely manifest as a more gradual change in the RSL curve which is not the case in the present study and does not explain the return to higher RSL or the oscillations reported elsewhere on the AEC.

Climate and sea level

Evidence of rapid climate change events during the Holocene is abundant, and although attempts to reconcile a global Holocene climate signal have been made (Bond et al. 1997, 2001; Mayewski et al. 2004; Wanner et al. 2011, 2015), the currently available records are significantly biased to the northern hemisphere, with continuous high-resolution records from the southern hemisphere relatively sparse (Wanner et al. 2015). Furthermore, whether rapid (subcentennial to centennial) shifts in climate translated to either minor relative or eustatic SL variability is difficult to ascertain and rarely discussed. Hamanaka et al. (2012) interpreted reef hiatus events in the mid-Holocene at Kodakara Island in the northwest Pacific as associated with oscillations in RSL, and suggested links to possible eustatic oscillations driven by Atlantic and Pacific cold events and associated short-lived ice build-up. Similarly, links between climate perturbations and SL oscillations in the Atlantic at ~6500 and 2200 yr BP (Schellmann and Radtke 2010) and in the Pacific in response to the "Little

Climatic Optimum" and "Little Ice Age" of the late Holocene have also been proposed (Nunn 1998, 2000a, b). Conversely, glacio-isostatically adjusted mangrove and reef deposit data from the Seychelles (Indian Ocean) suggest that ESL has been largely insensitive to climate fluctuations over the past 2000 yr prior to anthropogenic influence (Woodroffe et al. 2015). Although a recent re-analysis of available "far-field" sea level data by Lambeck et al. (2014) concluded that no oscillations of >0.2 m occurred during the last 6000 yr, this conclusion is limited to timescales of ≥200 yr due to age uncertainties, which is above the temporal detection limit of the oscillations presented here for the Keppel Islands. Unfortunately, insufficient continuous high-resolution climate data in the southern hemisphere (Wanner et al. 2011, 2015) make interpretation of Holocene regional and global climate signals on SL variability tenuous. Coral proxy-derived (Sr/Ca and $\delta^{18}O$) sea surface temperature (SST) data from Orpheus Island and King Reef in the northern GBR suggest that SSTs were ~1.0–1.2 °C warmer than present at ~ 5300 (Gagan et al. 1998) and 4700 yr BP (Roche et al. 2014). Warmer SSTs have also been inferred from foraminiferal $\delta^{18}O$ analysis from near Indonesia, with warm/wet and stable conditions prior to 5500–5300 yr BP (Brijker et al. 2007). Conversely, coral data from Indonesia and Papua New Guinea suggest a cooling of ~1.2 °C at ~5500 yr BP (Abram et al. 2009). With consideration of the age errors in these records, a possible 1.0–2.0 °C change in SST affecting the Indo-Pacific during the mid-Holocene is possible; however, this cannot be validated with the data currently available.

Nevertheless, in this study, we have demonstrated that by using high-precision U–Th dating techniques, in conjunction with elevation surveys of a single SL indicator at multiple sites, it is possible to detect minor (<1 m) RSL fluctuations. The RSL oscillations presented here for the Keppel Islands are in good temporal agreement with episodes of significant change to reefs on the GBR throughout the Holocene ("turn-off" and hiatus). With current models predicting a 0.2- to 0.6-m contribution to sea level rise for each 1 °C of global warming in the future (Church et al. 2013) is it not then possible that similar scale cooling events in the Holocene had comparable effects on at least RSL signals in the far-field? Given the rates and magnitudes of change in the present study, and lack of evidence for any other geological or geomorphological contributions, we consider significant subcentennial to centennial climate perturbations the most likely driver of RSL oscillations in the Keppel Islands. Clearly, more high-resolution RSL records are needed to determine whether this is a local, regional or global signal, and robust links to possible climate perturbations are required before any further conclusions can be drawn.

High-resolution palaeo-sea level reconstructions are not only critical to interpreting reef growth history on the GBR, but will enable improved predictions of reef response to future SL variability (Camoin and Webster 2015). Further, precisely dated RSL records in conjunction with high-resolution palaeo-climate data will enable refinement to model parameters for use in future sea level rise projections.

Acknowledgments We thank C. Murray-Wallace and one anonymous reviewer for their comments which improved this manuscript. Also Hannah Markham, Mauro Lepore, Martina Prazeres, Ian Butler and others involved in fieldwork, the crew of MV Adori, and A.D. Nguyen. This study was funded by the National Environmental Research Programme Tropical Ecosystems Hub Project 1.3 to J-xZ, JMP, SGS, TRC, Y-xF and others, Australian Research Council Linkage, Infrastructure, Equipment and Facilities (LIEF) grant (LE0989067 for the MC-ICP-MS) to J-xZ, JMP, Y-xF and others, and an Australian Postgraduate Award to NDL. Samples were collected under permit G12/34,979.1.

References

Abram NJ, McGregor HV, Gagan MK, Hantoro WS, Suwargadi BW (2009) Oscillations in the southern extent of the Indo-Pacific Warm Pool during the mid-Holocene. Quat Sci Rev 28:2794–2803

Baker R (2001) Inter-tidal fixed indicators of former Holocene sea levels in Australia: a summary of sites and a review of methods and models. Quat Int 83–85:257–273

Baker R, Haworth RJ (2000) Smooth or oscillating late Holocene sea-level curve? Evidence from the palaeo-zoology of fixed biological indicators in east Australia and beyond. Mar Geol 163:367–386

Bond G, Bonani G, Showers W, Cheseby M, Lotti R, Almasi P, deMenocal P, Priore P, Cullen H, Hajdas I (1997) A pervasive millennial-scale cycle in North Atlantic Holocene and glacial climates. Science 278:1257–1266

Bond G, Bonani G, Kromer B, Beer J, Muscheler R, Evans MN, Showers W, Hoffmann S, Lotti-Bond R, Hajdas I (2001) Persistent solar influence on North Atlantic climate during the Holocene. Science 294:2130–2136

Brijker JM, Jung SJA, Ganssen GM, Bickert T, Kroon D (2007) ENSO-related decadal scale climate variability from the Indo-Pacific Warm Pool. Earth Planet Sci Lett 253:67–82

Brooke B, Ryan D, Pietsch T, Olley J, Douglas G, Packett R, Radke L, Flood P (2008) Influence of climate fluctuations and changes in catchment land use on late Holocene and modern beach-ridge sedimentation on a tropical macrotidal coast: Keppel Bay, Queensland, Australia. Mar Geol 251:195–208

Buddemeier RW, Hopley D (1988) Turn-ons and turn-offs: causes and mechanisms of the initiation and termination of coral reef growth. Proc 6th Int Coral Reef Symp 1:253–261

Bureau of Meteorology (2011) Australian climate variability and change — time series graphs. Australian Bureau of Meteorology, Commonwealth of Australia. http://www.bom.gov.au/climate

Camoin GF, Webster JM (2015) Coral reef response to Quaternary sea-level and environmental changes: state of the science. Sedimentology 62:401–428

Chappell J (1983) Evidence for smoothly falling sea-level relative to North Queensland, Australia, during the past 6,000 yr. Nature 302:406–408

Chappell J, Rhodes EG, Thom BG, Wallensky E (1982) Hydro-isostasy and the sea-level isobase of 5500 B.P. in north Queensland. Australia. Mar Geol 49:81–90

Cheng H, Edwards RL, Hoff J, Gallup CD, Richards DA, Asmerom Y (2000) The half-lives of uranium-234 and thorium-230. Chem Geol 169:17–33

Church JA, Clark PU, Cazenave A, Gregory JM, Jevrejeva S, Levermann A, Merrifield MA, Milne GA, Nerem RS, Nunn PD, Payne AJ, Pfeffer WT, Stammer D, Unnikrishnan AS (2013) Sea level change. In: Stocker TF, Qin D, Plattner G-K, Tignor M, Allen SK, Boschung J, Nauels A, Xia Y, Bex V, Midgley PM (eds) Climate change 2013: the physical science basis. Contribution of working group I to the fifth assessment report of the Intergovernmental Panel on Climate Change, Cambridge, UK and New York, NY, USA, pp 1137–1186

Clark JA, Farrell WE, Peltier WR (1978) Global changes in postglacial sea level: a numerical calculation. Quat Res 9:265–287

Clark TR, Roff G, J-x Zhao, Y-x Feng, Done TJ, Pandolfi JM (2014a) Testing the precision and accuracy of the U-Th chronometer for dating coral mortality events in the last 100 years. Quat Geochronol 23:35–45

Clark TR, J-x Zhao, Y-x Feng, Done TJ, Jupiter S, Lough J, Pandolfi JM (2012) Spatial variability of initial ^{230}Th/^{232}Th in modern Porites from the inshore region of the Great Barrier Reef. Geochem Cosmochim Acta 78:99–118

Clark TR, J-x Zhao, Roff G, Y-x Feng, Done TJ, Nothdurft LD, Pandolfi JM (2014b) Discerning the timing and cause of historical mortality events in modern *Porites* from the Great Barrier Reef. Geochim Cosmochim Acta 138:57–80

Cobb KM, Charles CD, Cheng H, Kastner M, Edwards RL (2003) U/Th-dating living and young fossil corals from the central tropical Pacific. Earth Planet Sci Lett 210:91–103

Flood PG, Frankel E (1989) Late Holocene higher sea level indicators from eastern Australia. Mar Geol 90:193–195

Gagan MK, Ayliffe LK, Hopley D, Cali J, Mortimer G, Chappell J, McCulloch MT, Head M (1998) Temperature and surface-ocean water balance of the mid-Holocene tropical western Pacific. Science 279:1014–1018

Hamanaka N, Kan H, Yokoyama Y, Okamoto T, Nakashima Y, Kawana T (2012) Disturbances with hiatuses in high-latitude coral reef growth during the Holocene: correlation with millennial-scale global climate change. Glob Planet Change 80–81:21–35

Harris DL, Webster JM, Vila-Concejo A, Hua Q, Yokoyama Y, Reimer PJ (2015) Late Holocene sea-level fall and turn-off of reef flat carbonate production: rethinking bucket fill and coral reef growth models. Geology 43:175–178

Henderson GM (2002) Seawater (^{234}U/ ^{238}U) during the last 800 thousand years. Earth Planet Sci Lett 199:97–110

Hopley D (1980) Mid-Holocene high sea levels along the coastal plain of the Great Barrier Reef Province: A discussion. Mar Geol 35:M1–M9

Hopley D, Smithers SG, Parnell K (2007) The geomorphology of the Great Barrier Reef: development, diversity and change. Cambridge University Press, Cambridge

Hua Q, Webb GE, J-x Zhao, Nothdurft LD, Lybolt M, Price GJ, Opdyke BN (2015) Large variations in the Holocene marine radiocarbon reservoir effect reflect ocean circulation and climatic changes. Earth Planet Sci Lett 422:33–44

Hughes TP, Connell JH (1999) Multiple stressors on coral reefs: a long-term perspective. Limnol Oceanogr 44:932–940

Kennedy DM, Woodroffe CD (2002) Fringing reef growth and morphology: a review. Earth Sci Rev 57:255–277

Kleypas JA, Hopley D (1992) Reef development across a broad continental shelf, southern Great Barrier Reef, Australia. Proc 7th Int Coral Reefs Symp 2:1129–1141

Lambeck K (1993) Glacial rebound and sea-level change: an example of a relationship between mantle and surface processes. Tectonophysics 223:15–37

Lambeck K (2002) Sea level change from mid Holocene to recent time: an Australian example with global implications. Geodynamics Series 29:33–50

Lambeck K, Nakada M (1990) Late Pleistocene and Holocene sea-level change along the Australian coast. Palaeogeog Palaeoclimatol Palaeoecol 89:143–176

Lambeck K, Rouby H, Purcell A, Sun Y, Sambridge M (2014) Sea level and global ice volumes from the Last Glacial Maximum to the Holocene. Proc Natl Acad Sci U S A 111:15296–15303

Larcombe P, Woolfe KJ (1999) Terrigenous sediments as influences upon Holocene nearshore coral reefs, central Great Barrier Reef, Australia. Aust J Earth Sci 46:141–154

Leonard ND, Welsh KJ, J-x Zhao, Nothdurft LD, Webb GE, Major J, Y-x Feng, Price GJ (2013) Mid-Holocene sea-level and coral reef demise: U-Th dating of subfossil corals in Moreton Bay, Australia. The Holocene 23:1841–1852

Lewis SE, Wu RAJ, Webster JM, Shields GA (2008) Mid-late Holocene sea-level variability in eastern Australia. Terra Nova 20:74–81

Lewis SE, Sloss CR, Murray-Wallace CV, Woodroffe CD, Smithers SG (2013) Post-glacial sea-level changes around the Australian margin: a review. Quat Sci Rev 74:115–138

Ludwig KR (2003) Isoplot/Ex, version 3: a geochronological toolkit for Microsoft Excel. Berkeley Geochronology Center Special Publications, Berkeley, CA, USA

Lybolt M, Neil DT, Zhao J, Feng Y, Yu K, Pandolfi J (2011) Instability in a marginal coral reef: the shift from natural variability to a human-dominated seascape. Front Ecol Environ 9:154–160

Mayewski PA, Rohling EE, Stager JC, Karlén W, Maasch KA, Meeker DL, Meyerson EA, Gasse F, van Kreveld S, Holmgren K, Lee-Thorp J, Rosqvist G, Rack F, Staubwasser M, Schneider RR, Steig EJ (2004) Holocene climate variability. Quat Res 62:243–255

McGregor HV, Gagan MK, McCulloch MT, Hodge E, Mortimer G (2008) Mid-Holocene variability in the marine ^{14}C reservoir age for northern coastal Papua New Guinea. Quat Geochronol 3:213–225

Mitrovica JX, Milne GA (2002) On the origin of late Holocene sea-level highstands within equatorial ocean basins. Quat Sci Rev 21:2179–2190

Murray-Wallace CV, Woodroffe CD (2014) Quaternary sea-level changes: a global perspective. Cambridge University Press, Cambridge, New York

Nakada M, Lambeck K (1989) Late Pleistocene and Holocene sea-level change in the Australian region and mantle rheology. Geophys J In 96:497–517

Narayan YR, Lybolt M, J-x Zhao, Feng Y, Pandolfi JM (2015) Holocene benthic foraminiferal assemblages indicate long-term marginality of reef habitats from Moreton Bay, Australia. Palaeogeog Palaeoclimatol Palaeoecol 420:49–64

Neumann AC, Macintyre IG (1985) Reef response to sea level rise: keep-up, catch up or give-up. Proc 5th Int Coral Reef Symp 3:105–110

Nunn PD (1998) Sea-level changes over the past 1,000 years in the Pacific. J Coast Res 14:23–30

Nunn PD (2000a) Environmental catastrophe in the Pacific Islands around A.D. 1300. Geoarchaeology 15:715–740

Nunn PD (2000b) Illuminating sea-level fall around AD 1220–1510 (730–440 cal yr BP) in the Pacific Islands: implications for environmental change and cultural transformation. N Z Geog 56:46–54

Pandolfi JM, Bradbury RH, Sala E, Hughes TP, Bjorndal KA, Cooke RG, McArdle D, McClenachan L, Newman MJH, Paredes G, Warner RR, Jackson JBC (2003) Global trajectories of the long-term decline of coral reef ecosystems. Science 301:955–958

Perry C, Smithers S (2011) Cycles of coral reef 'turn-on', rapid growth and 'turn-off' over the past 8500 years: a context for understanding modern ecological states and trajectories. Glob Chang Biol 17:76–86

Pirazzoli PA, Pluet J (1991) World atlas of Holocene sea-level changes. Elsevier, Amsterdam, New York

Roche RC, Perry CT, Smithers SG, Leng MJ, Grove CA, Sloane HJ, Unsworth CE (2014) Mid-Holocene sea surface conditions and riverine influence on the inshore Great Barrier Reef. The Holocene 24:885–897

Rodriguez-Ramirez A, Grove CA, Zinke J, Pandolfi JM, J-x Zhao (2014) Coral luminescence identifies the Pacific decadal oscillation as a primary driver of river runoff variability impacting the southern Great Barrier Reef. PloS One 9:e84305

Schellmann G, Radtke U (2010) Timing and magnitude of Holocene sea-level changes along the middle and south Patagonian Atlantic coast derived from beach ridge systems, littoral terraces and valley-mouth terraces. Earth Sci Rev 103:1–30

Scoffin TP, Stoddart DR, Rosen BR (1978) The nature and significance of microatolls. Phil Trans R Soc Lond B Biol Sci 284:99–122

Shen C-C, Fan T-Y, Meltzner AJ, Taylor FW, Quinn TM, Chiang H-W, Kilbourne KH, Li K-S, Sieh K, Natawidjaja D, Cheng H, Wang X, Edwards RL, Lam DD, Hsieh Y-T (2008) Variation of initial 230Th/ 232Th and limits of high precision U-Th dating of shallow-water corals. Geochim Cosmochim Acta 72:4201–4223

Sloss CR, Murray-Wallace CV, Jones BG (2007) Holocene sea-level change on the southeast coast of Australia: a review. The Holocene 17:999–1014

Smithers SG, Woodroffe CD (2000) Microatolls as sea-level indicators on a mid-ocean atoll. Mar Geol 168:61–78

Smithers SG, Hopley D, Parnell KE (2006) Fringing and nearshore coral reefs of the Great Barrier Reef: episodic Holocene development and future prospects. J Coast Res 2006:175–187

Toth LT, Macintyre IG, Aronson RB, Vollmer SV, Hobbs JW, Urrego DH, Cheng H, Enochs IC, Combosch DJ, van Woesik R (2012) ENSO drove 2500-year collapse of eastern Pacific coral reefs. Science 337:81–84

Veron JEN, Hoegh-Guldberg O, Lenton TM, Lough JM, Obura DO, Pearce-Kelly P, Sheppard CRC, Spalding M, Stafford-Smith MG, Rogers AD (2009) The coral reef crisis: the critical importance of $<$350 ppm CO_2. Mar Pollut Bull 58:1428–1436

Wanner H, Mercolli L, Grosjean M, Ritz SP (2015) Holocene climate variability and change: a data-based review. J Geol Soc London 172:254–263

Wanner H, Solomina O, Grosjean M, Ritz SP, Jetel M (2011) Structure and origin of Holocene cold events. Quat Sci Rev 30:3109–3123

Woodroffe CD, Horton BP (2005) Holocene sea-level changes in the Indo-Pacific. J Asian Earth Sci 25:29–43

Woodroffe CD, Kennedy DM, Hopley D, Rasmussen CE, Smithers SG (2000) Holocene reef growth in Torres Strait. Mar Geol 170:331–346

Woodroffe SA (2009) Testing models of mid to late Holocene sea-level change, North Queensland, Australia. Quat Sci Rev 28:2474–2488

Woodroffe SA, Long AJ, Milne GA, Bryant CL, Thomas AL (2015) New constraints on late Holocene eustatic sea-level changes from Mahé, Seychelles. Quat Sci Rev 115:1–16

Yu KF, Zhao JX (2010) U-series dates of Great Barrier Reef corals suggest at least +0.7 m sea level similar to 7000 years ago. The Holocene 20:161–168

Yu K, Hua Q, Zhao J-x, Hodge E, Fink D, Barbetti M (2010) Holocene marine ^{14}C reservoir age variability: evidence from ^{230}Th-dated corals in the South China Sea. Paleoceanography 25 (doi:10.1029/2009PA001831)